Factor XIII activation peptide is released into plasma upon cleavage by thrombin and shows a different structure compared to its bound form

Verena Schroeder[1], Jean-Marc Vuissoz[2], Amedeo Caflisch[3], Hans P. Kohler[1]

[1]Laboratory for Thrombosis Research, Department of Clinical Research, University of Bern, Bern, Switzerland; [2]Pediatric Endocrinology and Metabolism, University Children's Hospital, Inselspital, Bern, Switzerland; [3]Computational Structural Biology, Department of Biochemistry, University of Zurich, Zurich, Switzerland

Summary

The first step of coagulation factor XIII (FXIII) activation involves cleavage of the FXIII activation peptide (FXIII-AP) by thrombin. However, it is not known whether the FXIII-AP is released into plasma upon cleavage or remains attached to activated FXIII. The aim of the present work was to study the structure of free FXIII-AP, develop an assay for FXIII-AP determination in human plasma, and to answer the question whether FXIII-AP is released into plasma. We used ab-initio modeling and molecular dynamics simulations to study the structure of free FXIII-AP. We raised monoclonal and polyclonal antibodies against FXIII-AP and developed a highly sensitive and specific ELISA method for direct detection of FXIII-AP in human plasma. Structural analysis showed a putative different conformation of the free FXIII-AP compared to FXIII-AP bound to the FXIII protein. We concluded that it might be feasible to develop specific antibodies against the free FXIII-AP. Using our new FXIII-AP ELISA, we found high levels of FXIII-AP in in-vitro activated plasma samples and serum. We showed for the first time that FXIII-AP is detached from activated FXIII and is released into plasma, where it can be directly measured. Our findings may be of major clinical interest in regard to a possible new marker in thrombotic disease.

Keywords

Factor XIII, activation peptide, activation marker, molecular dynamics simulations

Thromb Haemost 2007; 97: 890–898

Introduction

Activated blood coagulation factor XIIIa (FXIIIa), which is a transglutaminase, covalently cross-links fibrin polymers and incorporates antifibrinolytic proteins into fibrin. In consequence of these reactions, the fibrin clot obtains sufficient stability and resistance to premature fibrinolysis (1, 2). According to these functions in clot formation, FXIII is a major player in any thrombo-embolic event, namely myocardial infarction, ischemic stroke, deep vein thrombosis, and pulmonary embolism (3–6).

FXIII zymogen circulates in plasma as a tetramer of two catalytic A-subunits and two carrier B-subunits (A_2B_2). In plasma, thrombin initiates the physiological conversion of the FXIII zymogen into the active enzyme by cleavage of the N-terminal activation peptide (AP), resulting in FXIII A'_2B_2. This reaction is greatly enhanced by fibrin. Then, the dissociation of the A'- and B-subunits is induced by conformational changes due to the binding of Ca^{2+}, again enhanced by fibrin. Finally, in the absence of the B-subunits and in presence of Ca^{2+}, the A'-subunits assume their active configuration (A*) (7).

Despite the increasing interest in FXIII, its numerous functions, and its role in various diseases, several issues, in particular regarding FXIII activation, have not been resolved yet. It is not known whether the AP cleaved from plasmatic FXIII is actually released or remains associated with the activated protein *in vivo*. In the 1970s, Schwartz et al. (8) showed the electrophoretic pat-

Correspondence to:
Prof. Hans-Peter Kohler
Laboratory for Thrombosis Research
Department of Clinical Research
Kinderklinik G3, Room 835
Inselspital, University Hospital of Bern
3010 Bern, Switzerland
Tel.: +41 31 632 9549, Fax: +41 31 632 2683
E-mail: hanspeter.kohler@spitalnetzbern.ch

Financial support:
This work was funded by the Swiss National Science Foundation (Grant No. 3200B0–105385).

Received August 22, 2006
Accepted after resubmission March 30, 2007

Prepublished online May 3, 2007
doi:10.1160/TH06–08–0458

terns of non-activated and activated FXIII on polyacrylamide gels in sodium dodecyl sulfate. When activated by thrombin, the A-subunit decreases in molecular weight by 4,000, indicating release of the AP. From the first three-dimensional structure of FXIII obtained from X-ray crystallography Yee et al. (9) deduced that the AP blocks the access to the active site cavity, and therefore important conformational changes including removal or at least movement of the AP are required for FXIII activation. Later, however, X-ray crystallography of the FXIII A'_2 dimer after cleavage of the AP by thrombin gave some evidence that the AP is not released, since no significant conformational changes in the protein were found, and the AP had almost the same conformation and occupied the same position as within the zymogen structure (10). On the conformation of the free AP itself, if released, nothing is known so far. Some evidence for the release of FXIII-AP after its cleavage comes from in-vitro experiments studying the kinetics of FXIII activation in purified systems, where free AP was detected by high-pressure liquid chromatography (HPLC) (11, 12). Another study has described mass spectrometric detection of the AP after extensive processing of serum samples (13). However, all experimental settings mentioned above involved special, non-physiological conditions, e.g. denaturating agents, high concentrations for crystallization, protein precipitation, chemical solvents, or high pressure. Therefore, these results may not apply to the situation *in vivo*. In summary, there exist no data whether or not the FXIII-AP is released under physiological conditions into plasma upon FXIII activation.

In the work we present here, we used ab-initio modeling and molecular dynamics simulations to study the structure of free FXIII-AP and compared its putative structure to FXIII-AP bound to the parent FXIII protein in order to investigate the theoretical feasibility of raising specific antibodies against FXIII-AP. We then produced specific antibodies against FXIII-AP and developed a sensitive and specific ELISA method for direct detection of circulating FXIII-AP. If the FXIII-AP is indeed released *in vivo*, this may be of major clinical interest since it could serve as a new marker for acute thrombotic disease.

Materials and methods

Structural analysis

Structural analysis was based on the crystal structure of the FXIII A_2-homodimer (14) obtained from the Protein Data Bank PDB (http://www.rcsb.org/pdb/; PDB Entry 1F13). The amino acid sequence of the FXIII-AP (amino acids 1–37) was submitted to the HMMSTR/Rosetta Prediction server (http://www.bioinfo.rpi.edu/~bystrc/hmmstr/server.php). This server uses ab-initio methods (I-sites, HMMSTR, and Rosetta) to determine the structure of the backbone. Coordinates of the side chain atoms were added using the CHARMM version 31b1 software with the CHARMM19 forcefield and EEF1 implicit solvation model (15, 16). The conformation generated *ab initio* by the HMMSTR/Rosetta server was not interpreted as a possible structure of the AP but was used solely as a starting conformation for MD simulations. Two other conformations were built using the same amino acid sequence of the FXIII-AP: a fully extended structure and a "crystal structure" by modeling the residues 1–4 and 37 which are not described in the FXIII A_2-homodimer crystal structure. Using these three different starting conformations, molecular dynamics (MD) simulations were performed to sample possible conformer(s) of the free AP.

First, a minimization of 5,000 steps using steepest descend followed by 500 steps of conjugate gradient was performed for all three structures. MD simulations were carried out using the implicit solvent forcefield EEF1/CHARMM19 parameters. The shake algorithm was used to restrain the hydrogen bonds and a time step of 2 fs was used. The system was heated from 1 K to a final temperature of 300 K increasing the temperature of 0.5 K every 6,000 steps. The MD simulations were then performed further with a time step of 2 fs at 300 K.

Analysis of the secondary structure was performed with STRIDE (17). Figures were produced with PyMOL (18) and VMD (19).

Antibody production

We developed antibodies against FXIII-AP in collaboration with ABGENT Inc. (San Diego, CA, USA). The detailed protocols can be accessed at http://www.abgent.com. In brief, the AP was synthesized according to the published sequence (SETSRT AFGGRRAVPPNNSNAAEDDLPTVELQGVVPR, PDB Entry 1F13). After HPLC purification, the AP was conjugated to keyhole limpet hemocyanin (KLH) as carrier protein. For production of polyclonal antibodies, two New Zealand White rabbits were repeatedly immunized, and several bleeds were taken between week 5 and week 10 after the first immunization. Antibody titers were determined by ELISA against the AP. The pooled bleeds were protein G affinity purified and affinity purified against the AP. Finally, we obtained 9 ml of purified antibody solution (0.31 mg/ml in phosphate-buffered saline) from one rabbit and 13 ml (0.49 mg/ml) from the other rabbit. Both polyclonal antibodies were tested against the free AP in reducing SDS-PAGE followed by Western blotting. We labeled 2 ml of the higher-concentrated polyclonal antibody with biotin using the EZ-Link® Sulfo-NHS-LC-Biotinylation Kit (Pierce, Rockford, IL, USA). For production of monoclonal antibodies against FXIII-AP, Balb/c mice were repeatedly immunized. After six weeks, the spleen cells from the mouse with the highest antibody titer were isolated and fused with myeloma cells. Clones were grown and tested by ELISA against FXIII-AP and FXIII protein. Clones that were positive against FXIII-AP and negative against FXIII protein were subcloned twice. The clone with the highest reactivity against FXIII-AP and the lowest reactivity against FXIII protein was selected for large-scale production with subsequent protein G affinity purification. Finally, we obtained 9 ml of purified monoclonal antibody (0.61 mg/ml in phosphate-buffered saline).

ELISA development

We developed a sandwich-type ELISA using either two polyclonal rabbit anti-FXIII-AP antibodies, one of them biotinylated, or a combination of one polyclonal and the monoclonal antibody. We applied the following assay procedure: Ninety-six-well microtiter plates (Maxisorp, Nunc, Roskilde, Denmark) were coated with 100 µl per well of the first polyclonal rabbit anti-FXIII-AP antibody (concentration 1 µg/ml in coating buffer con-

taining 50 mM sodium carbonate, pH 9.6). The plate was incubated at room temperature (RT) on a shaker for 1 hour (h), followed by overnight incubation at 4°C. After five washing steps with 200 µl of washing buffer (50 mM Tris-HCl, 150 mM NaCl, 0.1% Tween-20, 0.01% sodium azide, pH 7.5), we blocked the plate with 200 µl of blocking buffer (50 mM Tris-HCl, 150 mM NaCl, 1% bovine serum albumine, 0.01% sodium azide, pH 7.5) and incubated it at RT on a shaker for 1 h. After five washing steps, we diluted standards and plasma or serum samples appropriately with dilution buffer (50 mM Tris-HCl, 150 mM NaCl, 0.1% bovine serum albumine, 0.01% sodium azide, pH 7.5) and loaded 100 µl in duplicate onto the plate. After 1 h of incubation at RT on a shaker, we washed the plate five times, loaded either 100 µl of the biotinylated polyclonal rabbit anti-FXIII-AP antibody (1 µg/ml in dilution buffer) or 100 µl of the monoclonal mouse anti-FXIII-AP antibody (1 µg/ml in dilution buffer) onto the plate, and incubated it again for 1 h. After five washing steps, we loaded either 100 µl of streptavidine-alkaline-phosphatase conjugate (10 µg/ml in dilution buffer; Sigma, Fluka Chemie GmbH, Buchs, Switzerland) or 100 µl of goat anti-mouse IgG labelled with alkaline-phosphatase (1/1,000 in dilution buffer; Sigma, Fluka Chemie GmbH) onto the plate and incubated it again for 1 h. After five washing steps, we developed the plate with 100 µl of p-nitrophenyl phosphate (1 mg/ml in 1 M diethanolamine containing 0.5 mM $MgCl_2$, pH 9.8; Sigma) and incubated it at RT on a shaker. We stopped the color-developing reaction after exactly 10 minutes (min) with 100 µl of 4 M NaOH and measured optical density (OD) values on a microplate reader at 405 nm with a reference filter at 550 nm (Tecan SLT Rainbow Reader with Magellan Software V1.11, Tecan Austria GmbH, Grödig, Austria).

We assessed specificity and sensitivity of the novel ELISA method by measuring FXIII-AP dilutions in dilution buffer, FXIII-deficient plasma (congenital FXIII-deficient plasma with <1.0% FXIII as assessed by ELISA, Milan Analytica, La Roche, Switzerland), and normal pool plasma. The synthetic FXIII-AP was diluted to final concentrations ranging from 1 µg/ml to 10 pg/ml (256 nM to 2.6 pM) in dilution buffer, in FXIII deficient plasma (which was diluted 1/10 and 1/100), and in normal pool plasma (diluted 1/10 and 1/100). In each dilution series, we included a blank without FXIII-AP. From the resulting concentration versus OD curves, we deduced linear range and detection limit of the ELISA and defined the standard curve.

Determination of in vitro generated AP

Blood from healthy volunteers was drawn into 5-ml tubes (Monovette®, Sarstedt AG, Sevelen, Switzerland) containing 0.5 ml trisodium citrate solution (0.106 M) for plasma separation or clot activator beads for serum separation. We centrifugated the plasma tubes immediately at 2,000 g for 20 min and then separated the citrated plasma. Serum tubes were allowed to stand for 30 min before centrifugation (2,000 g, 20 min) to let coagulation proceed.

For in-vitro generation of AP, we activated citrated plasma with thrombin (Sigma) and stopped the reaction after different time points with the thrombin inhibitor Phe-Pro-Arg-chloromethylketone "PPACK" (Bachem, Bubendorf, Switzerland). We performed the experiment in two parallel series, once with and once without the fibrin polymerization inhibiting peptide Gly-Pro-Arg-Pro-amide acetate (GPRP; Bachem). We mixed 100 µl of citrated plasma with 50 µl of GPRP (5 mg/ml in tris-buffered saline, TBS) or with 50 µl of TBS for the series without GPRP. We activated with 50 µl of thrombin (10 U/ml in TBS) or added 50 µl of TBS for the non-activated control. We stopped the reactions after 1, 2, 3, 4, 6, 8, and 10 min by addition of 50 µl of PPACK (140 µg/ml). The clotted samples without GPRP were centrifugated at 2,000 g for 10 min, and the supernatant was separated. For the AP ELISA, we diluted the activated plasma samples 1/50 in dilution buffer.

After centrifugation of the serum samples, one aliquot of each serum sample was immediately analyzed, two other aliquots were kept for 4 h at 4°C in the fridge and at RT. Serum was diluted 1/50 in dilution buffer for the AP ELISA which was performed using either the two polyclonals or the polyclonal/monoclonal combination.

In all plasma and serum samples, we also determined FXIII A-subunit antigen levels by an in-house ELISA (20). FXIII A-subunit antigen levels are expressed as percentage of the WHO 1st International Standard Factor XIII Plasma (National Institute for Biological Standards and Control, NIBSC, Potters Bar, UK).

Analysis of plasma clots for trapped AP

We generated plasma clots by incubating normal citrated plasma with thrombin (final concentration 1.2 U/ml) and calcium chloride (final concentration 16 mM) for 2 h at 37°C. We washed the clots three times with 0.9% saline and then added Laemmli sample buffer containing 54 mg/ml dithiothreitol. After boiling for 5 min at 95°C and incubation for 30 min, the clots were dissolved and analyzed by SDS-PAGE and Western blotting. Synthetic AP was used as a positive control.

Antibody specificity towards synthetic and natural AP

For generation of natural AP, we used a purified system containing purified plasma FXIII (67.5 nM), thrombin (7.5 U/ml), calciumchloride (15 mM), and fibrinogen (6 mg/ml) (cofactor in FXIII activation). After incubation during 10 min at 37°C, the samples were centrifuged and the supernatant was measured by ELISA. A control sample without thrombin and calciumchloride and solutions of synthetic AP (67.5 nM and 135 nM) were analyzed by ELISA as well. The concentration of 135 nM AP corresponds to the release of two APs per FXIII tetramer, 67.5 nM correponds to the release of only one AP per FXIII tetramer. The ELISA was performed either with two polyclonals, one of them biotinylated, or with the polyclonal-monoclonal combination. We also analyzed different concentrations of synthetic AP and natural AP, derived in the above purified system, by SDS-PAGE and Western blotting.

Results

Structural analysis

Figures 1A and B show the conformation of the AP bound to the FXIII A_2 homodimer. In this structure, the amino acids 28–32 are involved in a β-strand, but no further regular element of secondary structure is observed. To investigate the conformation of the free AP, eight MD simulations were performed starting from the

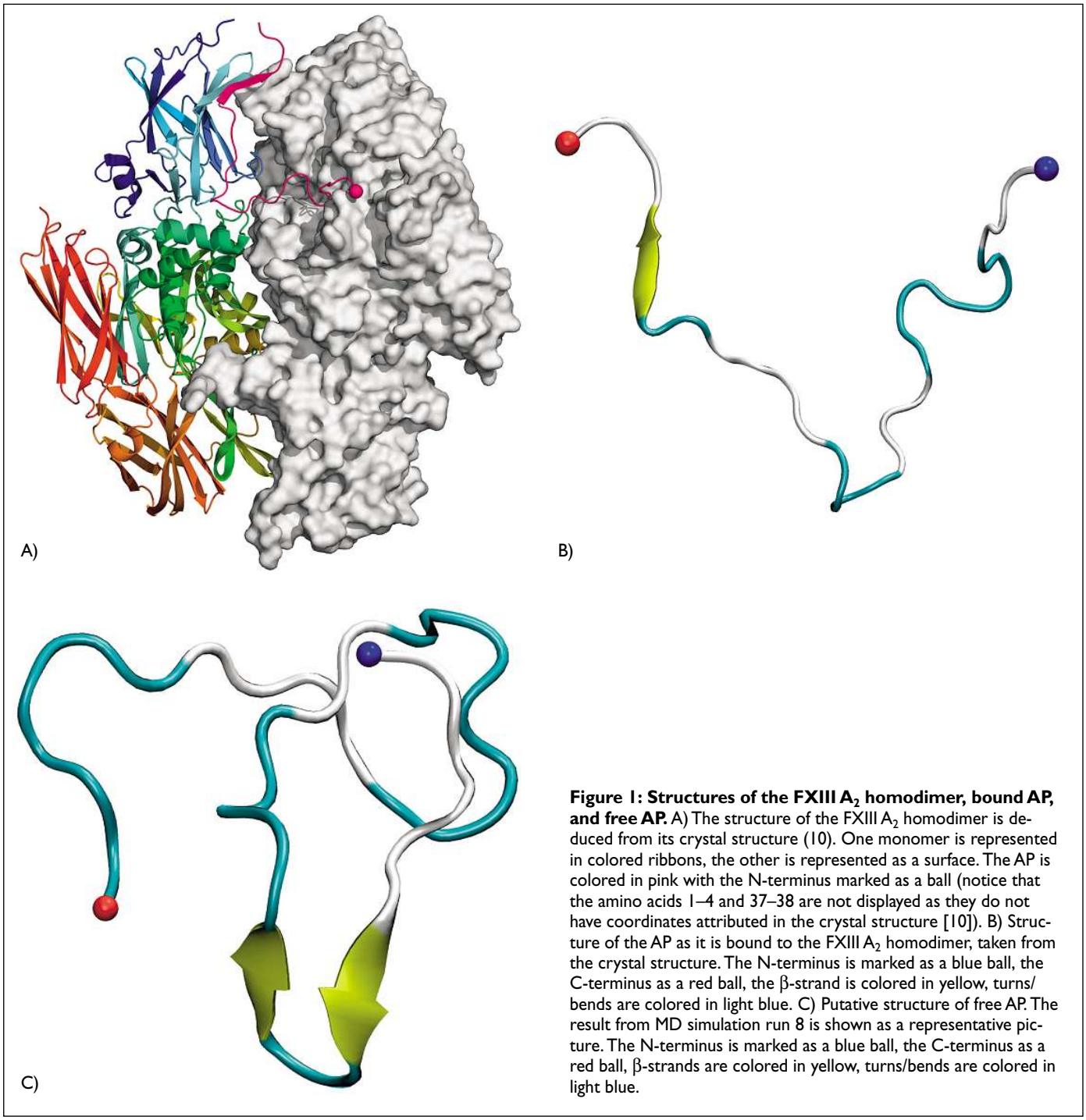

Figure 1: Structures of the FXIII A_2 homodimer, bound AP, and free AP. A) The structure of the FXIII A_2 homodimer is deduced from its crystal structure (10). One monomer is represented in colored ribbons, the other is represented as a surface. The AP is colored in pink with the N-terminus marked as a ball (notice that the amino acids 1–4 and 37–38 are not displayed as they do not have coordinates attributed in the crystal structure [10]). B) Structure of the AP as it is bound to the FXIII A_2 homodimer, taken from the crystal structure. The N-terminus is marked as a blue ball, the C-terminus as a red ball, the β-strand is colored in yellow, turns/bends are colored in light blue. C) Putative structure of free AP. The result from MD simulation run 8 is shown as a representative picture. The N-terminus is marked as a blue ball, the C-terminus as a red ball, β-strands are colored in yellow, turns/bends are colored in light blue.

crystal structure, a fully extended conformation, or a conformation predicted *ab initio* by the HMMSTR/Rosetta Prediction server (Table 1).

Starting from the crystal structure, the initial AP conformation was rapidly lost and β-strands were formed. In all MD simulations the conformation of the crystal structure was never sampled, and the final part of most trajectories had a high root mean square deviation (RMSD) from the homodimeric conformation and a higher β-strand content (Table 1), suggesting that the free AP does not assume the same structure as the AP within the FXIII A_2 homodimer. MD simulations starting from extended or ab initio modeled AP showed also a high tendency to form β-strands (Fig. 1C). At the end of the MD simulations, i.e. after 200 to 400 ns, all but one conformations had β-strands. In addition, some of the runs converged to the same β-strands structure. Figure 2 summarizes the average secondary structure content for each amino acid over all MD simulations.

The N-terminal amino acids 5 to 14 in the free AP showed a higher tendency to form β-strands than in the AP bound to non-activated FXIII. At the end of the MD simulations, six out of

No.	Starting conformation	Simulation length (nanoseconds)	Final conformation		
			RMSD (Angström)		β-structure (percent)
			crystal	modeled	
1	Crystal structure	300	14.0	12.1	16.2
2	Crystal structure	400	10.7	7.7	21.6
3	Fully extended peptide	300	14.1	9.3	16.2
4	Fully extended peptide	300	12.1	8.3	0
5	Modeled peptide	200	11.6	11.5	13.5
6	Modeled peptide	300	13.2	4.4	32.4
7	Modeled peptide	400	12.3	7.4	29.7
8	Modeled peptide	300	10.6	9.1	10.8

Table 1: Molecular dynamics simulations. The root mean square deviation (RMSD) of the Cα-atoms of the final snapshot was calculated at the end of each run. The reference conformation is either the crystal structure or the structure obtained by ab-initio modeling. Only the segment 5–36 is taken into account for the RMSD calculation because residues 1–4 and 37 are disordered and not present in the crystal structure (PDB ID 1F13). The β-structure content was evaluated for the final snapshot of each simulation. In comparison, the β-structure content of the AP in the homodimeric structure is about 13%.

eight structures had β-strands in this part of the free AP (Fig. 1C). This simulation result is of noticeable interest since these amino acids 5 to 14 of the AP are in close contact to the FXIII A_2 homodimer and may be involved in binding to the FXIII A_2 homodimer. By formation of β-strands in this part of the AP, the free AP may be prevented from binding to FXIII A_2.

In summary, the MD simulations indicated that the conformation of free FXIII-AP is likely to be different from the structure of the AP within the FXIII A_2 homodimer. Therefore, generation of antibodies specific for the free AP may be feasible and may represent a strategy to exploit the structural diversity between free and bound AP.

ELISA development and characterization

Rabbits and mice were successfully immunized with FXIII-AP, and a monoclonal and polyclonal antibodies could be generated and purified. The Western blot shown in Figure 3A confirmed the binding between the AP and polyclonal antibodies. We then developed an ELISA method which is based on the sandwich principle, using either two polyclonal antibodies or a polyclonal/monoclonal combination. The ELISA functions over a broad range of FXIII-AP concentration and is highly sensitive detecting AP concentrations as low as 0.01 ng/ml (2.6 pM). Figure 3A shows the AP concentration versus OD curves of the ELISA over a range of 0.01–100 ng/ml (2.6 pM – 25.6 nM) of AP diluted in dilution buffer, FXIII-deficient plasma, and normal pool plasma. The detection limit of the ELISA was 0.01 ng/ml (2.6 pM) in dilution buffer and 0.1 ng/ml (26 pM) in plasma (diluted at least 1/10). Furthermore, the ELISA is highly specific since dilution of AP in FXIII-deficient plasma and normal pool plasma gave similar curves to AP diluted in buffer, indicating that the antigen/antibody reaction is independent of the presence of other plasma components, including plasma FXIII. We were able to detect different AP concentrations in FXIII-deficient plasma and normal pool plasma as accurately as in dilution buffer. Blank values of the diluted plasmas were similar to the dilution buffer blank and gave no significant OD signals. Therefore, there is no cross-reactivity with tetrameric plasma FXIII. We finally defined representative standard curves of the ELISA, shown in Figure 3B, in the linear part of the concentration versus OD curve.

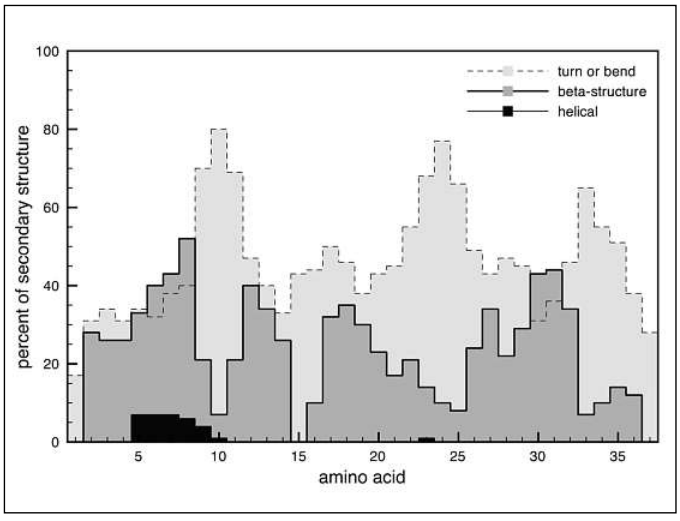

Figure 2: Average secondary structure content of free AP. The average secondary structure for each amino acid was calculated from all MD simulations (run 1–8). The first 100 ns of each run were omitted to prevent bias of the starting conformation. Most notably, the average secondary structure content, in particular β-structures and turns, was higher than in the homodimeric conformation.

Determination of AP generated *in vitro*

In non-activated citrated plasma samples from four healthy volunteers, we found FXIII A-subunit antigen levels of 114–147% (expressed as percentage of the International Standard FXIII Plasma), but we could not detect any FXIII-AP. In the serum samples from the same individuals, we measured high AP levels of 86–145 ng/ml (22–37 nM), as determined by both the polyclonal ELISA and also the polyclonal/monoclonal ELISA, and low FXIII A-subunit antigen levels of <1–4%. In the serum samples kept for 4 h at 4°C we still found 80% and in the samples kept at RT 65% of the original AP concentration.

Figure 4 shows the time course of FXIII-AP and FXIII A-subunit antigen levels after activation *in vitro* of citrated plasma. Without addition of the fibrin polymerization inhibiting peptide, we observed fast clot formation in the samples. This is re-

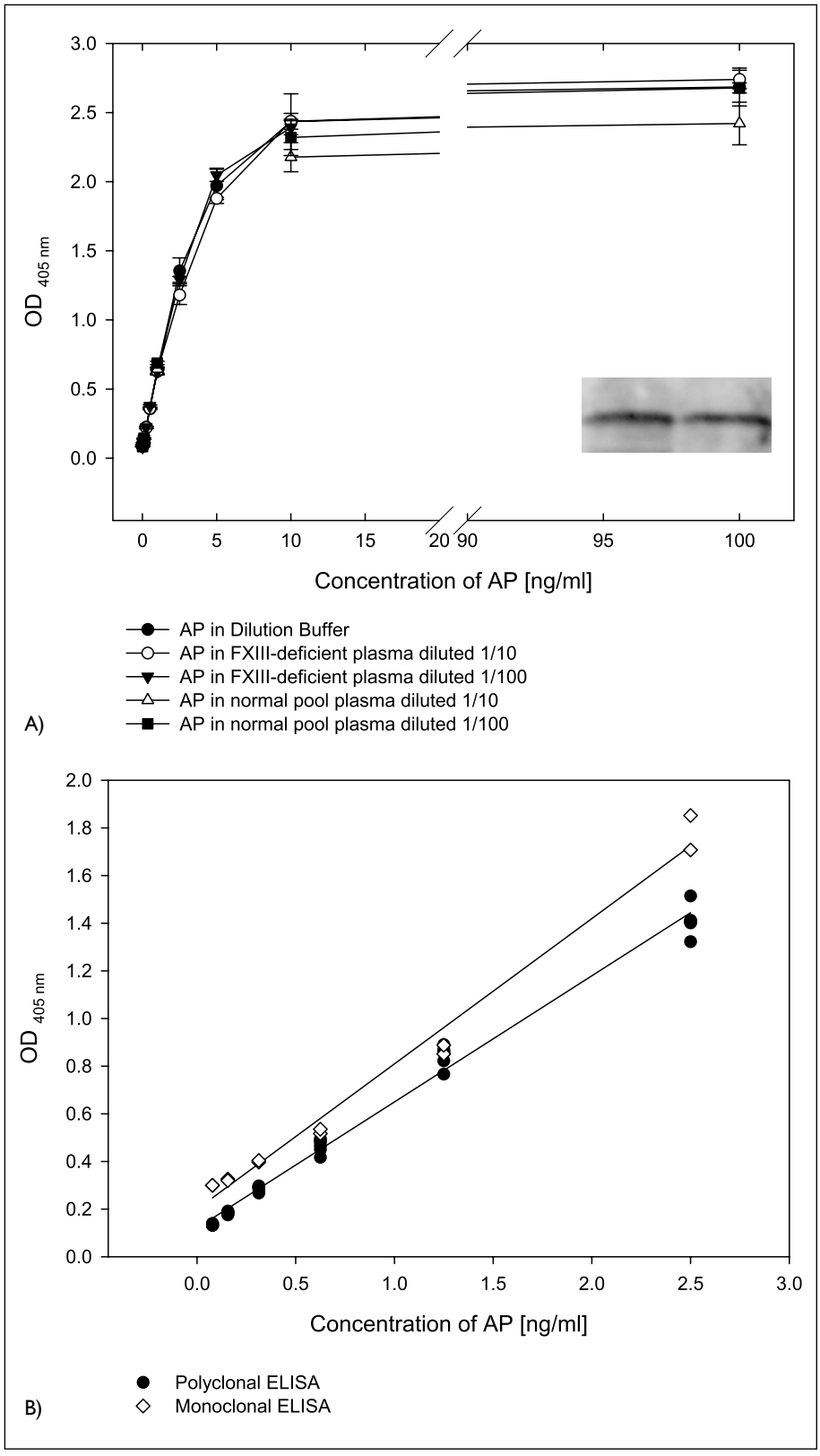

Figure 3: Characterization of the FXIII-AP ELISA. A) Concentration of AP versus OD. AP concentration ranged from 0.01–100 ng/ml (2.6 pM-26 nM) in dilution buffer, FXIII-deficient plasma, and normal pool plasma. (Mean values from duplicates with error bars representing standard deviation [SD] are shown.) The Western blot from reducing SDS-PAGE confirmed the binding between free AP and the polyclonal antibodies (a representative blot with one of the two polyclonals is displayed). B) Representative standard curves of the FXIII-AP ELISA using two polyclonal antibodies (black symbols representing individual values from six replicates) or a polyclonal/monoclonal combination (open symbols representing two replicates). The AP-concentrations of the six standards were as follows: 2.5, 1.25, 0.625, 0.3125, 0.15625, and 0.078125 ng/ml (0.64–0.2 nM). The equations of the standard curves were y=0.54015x +0.11408 with the linear correlation coefficient r^2=0.998 for the polyclonal ELISA and y=0.61003x+0.19934 with r^2=0.985 for the poly-monoclonal ELISA.

flected by the ELISA results showing a fast increase in FXIII-AP and a fast decrease in FXIII A-subunit (Fig. 4A). In samples without clot formation due to inhibition of fibrin polymerization, we found similar AP levels, a less prominent decrease in FXIII A-subunit antigen levels, and the changes occurred slightly slower (Fig. 4B).

On the Western blot of the solubilized plasma clots we could not detect any AP (data not shown).

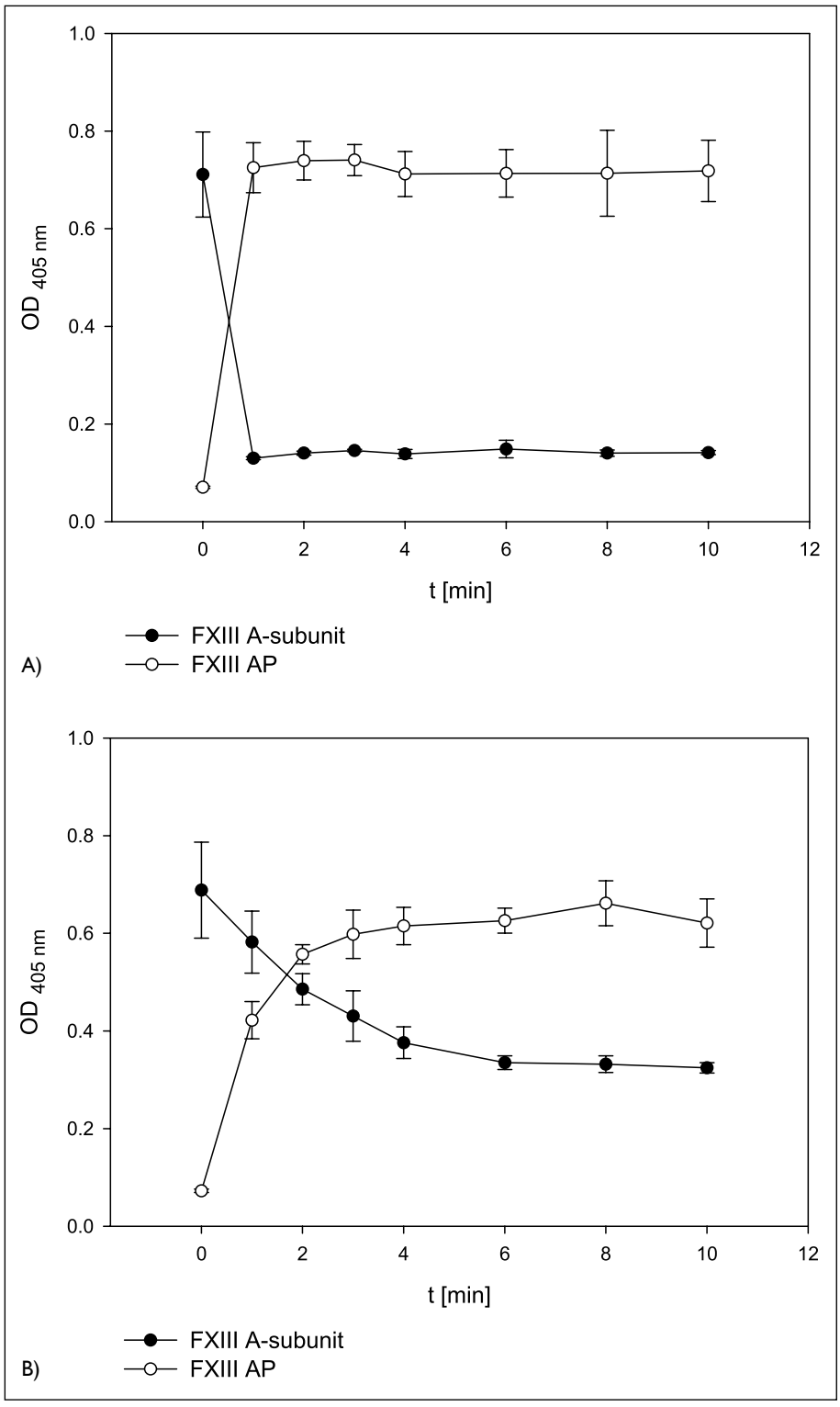

Figure 4: Time course of FXIII-AP and FXIII A-subunit antigen levels after in-vitro activation of citrated plasma. A) Without the fibrin polymerization inhibitor GPRP (mean values from three experiments with error bars representing SD). B) With GPRP (mean values from two experiments with error bars representing standard deviation).

Antibody specificity towards synthetic and natural AP

In order to investigate whether the antibodies might exhibit different specificities towards synthetic AP and natural AP generated by FXIII activation, we compared the ELISA signals of the same concentrations of synthetic and natural AP. In the ELISA using two polyclonal antibodies, we measured the following OD values (mean of two replicates): Synthetic AP (135 nM) OD 0.298, synthetic AP (67.5 nM) OD 0.184, natural AP (derived from 67.5 nM FXIII) OD 0.105. In the supernatant of the activated samples, the FXIII A-subunit was no longer detectable. Thus, compared to the synthetic AP, we measured 57% natural AP if one AP is released per FXIII tetramer, and 35% natural AP if two APs are released per FXIII tetramer. These results are consistent with our results obtained from activated plasma/serum

samples and indicate that the specificity of the polyclonal antibodies towards the natural AP is only half of the specificity towards the synthetic AP.

In the ELISA using the polyclonal/monoclonal combination, we measured the following OD values (mean of two replicates): Synthetic AP (135 nM) OD 0.328, synthetic AP (67.5 nM) OD 0.252, natural AP (derived from 67.5 nM FXIII) OD 0.207. Thus, compared to the synthetic AP, we measured 63% natural AP if two APs are released per FXIII tetramer, and even 82% natural AP if one AP is released per FXIII tetramer. These results may indicate that the Mab has a higher specificity towards natural AP than the Pabs, and that the Mab may be better than the Pabs for detecting natural AP.

When we visually compared synthetic and natural AP on a Western Blot (Fig. 5) we found that bands of synthetic AP showed a higher intensity than bands of natural AP in comparable concentrations. This result points again towards different specificities of the antibodies towards synthetic and natural AP and supports the results obtained by ELISA.

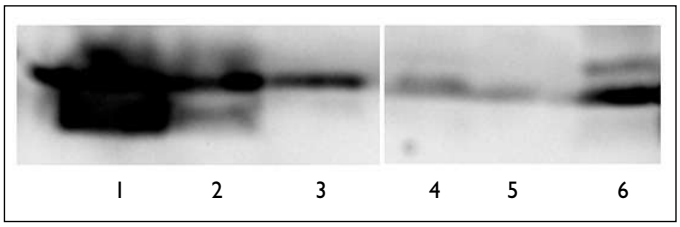

Figure 5: Antibody specificity towards synthetic and natural AP. Synthetic and natural AP were subjected to reducing SDS-PAGE and Western blotting using a polyclonal antibody. Concentrations of synthetic AP were (1) 5 µM, (2) 0.5 µM, (3) 0.05 µM, concentrations of natural AP were (4) 1 µM, (5) 0.4 µM, (6) 2 µM.

Discussion

For the first time, we show that upon activation by thrombin FXIII-AP is released into plasma where it can be directly quantified by a sensitive and specific ELISA method.

In our experiments, we avoided using a purified system to allow the best in vivo-like conditions, since the release of the activation peptide could depend on various cofactors which are only present in plasma. In addition, the use of plasma or serum avoids non-physiological reagents in the reaction mixture.

We compared the conformation of the AP bound to FXIII with the putative conformation of the free AP by using ab-initio modeling and MD simulation. A very similar implicit solvent MD simulation protocol in combination with the same force field employed here was shown in previous works to reproduce the NMR solution structure of a three-stranded antiparallel β-sheet peptide, irrespective of the starting conformation used in the MD runs (21). Moreover, the native structure of helical peptides and β-hairpin were reproduced correctly (22, 23). Therefore, the MD simulation method which was applied here to sample the conformation space of the free FXIII-AP is to be considered as suitable and valid. We observed conformational differences between the free AP showing two-stranded antiparallel β-sheet structures and the bound AP which has only one β-strand but no further secondary structures. These results were obtained consistently from repeated MD simulations and from different MD simulations using different starting conformations. Therefore, we conclude that our results describing the structure of the free AP are strongly supported, but still remain to be confirmed by nuclear magnetic resonance (NMR) studies.

The structural considerations led us to the assumption that the conformations of the two FXIII-AP forms are different *in vivo*. We concluded that it may be feasible to raise antibodies which are specific for the free FXIII-AP, provided that animals develop an immune response to the AP. Indeed, we obtained one monoclonal and two polyclonal antibodies against FXIII-AP that do not cross-react with the non-activated FXIII molecule in plasma, and this enabled us to develop the first immunologic assay for FXIII-AP detection. In a next step, we intend to develop further monoclonal antibodies and to characterize the antigen/antibody reactions by epitope mapping.

As shown, our FXIII-AP ELISA is highly sensitive. The standard curve was set in a very low range of FXIII-AP concentrations. This should enable us to detect even lowest amounts of FXIII-AP circulating *in vivo*. If massive amounts of FXIII-AP were generated during acute thrombotic events, the samples can be diluted. Furthermore, our FXIII-AP ELISA is highly specific, since we observed no cross-reactivity with tetrameric FXIII in plasma. Theoretically it could be possible that after activation and subsequent removal of the B-subunits a new epitope on the A-subunit is presented which then cross-reacts with our antibody. However, this is rather unlikely, since after FXIII activation and dissociation of the subunits, the FXIII A-subunit is trapped inside the forming clot where the cross-linking reaction takes place and activated FXIII (FXIIIa) remains associated with fibrin (24).

We can now answer the questions on the AP's fate after FXIII activation in plasma: Both after plasma FXIII activation by thrombin and after contact activation of the coagulation cascade to gain serum, high FXIII-AP levels can be measured in plasma/serum. At the same time, only traces of the FXIII A-subunit antigen can be detected after activation. This is consistent with the observations that activated FXIII tightly binds to fibrin, becomes incorporated into the clot and is removed from circulation, and therefore no or hardly any FXIII remains in the serum (24). When we prevented clot formation by addition of GPRP peptide, we found almost the same levels of AP, but there was still some FXIII A-subunit antigen detectable. These findings demonstrate that the FXIII-AP is released into plasma/serum and does not remain attached to its parent protein. If that were the case, we would expect to find only traces of AP in clotted samples, with the AP sticking to activated FXIII trapped within the fibrin network, but higher AP levels in the non-clotted GPRP samples. Furthermore, polymerized fibrin is obviously not necessary for release of FXIII-AP, since we measured FXIII-AP in the presence of the fibrin polymerization inhibitor GPRP.

The stoichiometry of FXIII activation and AP detection remains to be investigated more closely. In fully activated serum we measured 22–37 nM of FXIII-AP. Under the assumption that both APs per FXIII tetramer are released during FXIII activation, this corresponds to only approximately 25% of the normal FXIII

A-subunit plasma concentration of 130–160 nM (25). However, a previous study showed that cleavage of only one AP per FXIII molecule would be sufficient for complete activation of platelet FXIII (26). Thus, if only one AP per FXIII molecule is released and this is also applicable for tetrameric plasma FXIII, then our AP levels measured in serum and activated plasma would correspond to approximately 50% of FXIII plasma concentration.

In order to investigate if large amounts of cleaved FXIII-AP might remain trapped inside the fibrin clot, we solubilized plasma clots and analyzed them by SDS-PAGE and Western blotting. Since we found no AP inside the clot, we abandoned this possibility.

Another explanation may be due to the secondary structure of the AP. Analysis of its putative secondary structure showed that certain amino acids probably assume certain preferred secondary structures (which putatively distinguishes the structure of the free AP from the bound AP), but it also showed that other segments may be quite flexible. This flexibility may be a reason why some epitopes of the AP may not always be exposed and available for antibody binding.

For quantitation we made the standard curve of our ELISA with synthetic AP, which also served as immunogen in antibody production. However, there may be differences between the synthetic AP and the natural AP generated *in vitro* or *in vivo* during FXIII activation. Such differences may include posttranslational modifications. It has been described that the N-terminal serine of the AP is acetylated, and that asparagine 17 is a potential glycosylation site (24). Because of such differences, our antibodies might recognize the synthetic AP better than the natural AP, leading to underestimation of the natural AP. Our experiments comparing antibody specificity revealed that differences in specificity towards synthetic AP versus natural AP may indeed represent a major explanation for the underestimation of FXIII-AP in fully activated serum. Using a monoclonal antibody we were able to detect even up to >80% of natural AP compared to synthetic AP. Therefore, the detection rate of natural AP can surely be increased by further optimisation of the antibodies, targeting at a higher specificity towards the natural AP.

Further reasons for the observed discrepancy may be incomplete FXIII activation, adsorption to other plasma or serum proteins, or proteolytic degradation of the FXIII-AP. However, our experiments do provide sufficient evidence that a significant amount of FXIII-AP is released into plasma after activation of the zymogen, where it can be quantified.

Being reasonably stable over several hours, the FXIII-AP fulfills one of the prerequisits of a diagnostic marker and should therefore be measurable in fresh plasma samples for diagnosis of acute thrombotic events, similar to D-dimer testing.

We hypothesize that FXIII-AP may represent a novel marker in acute thrombotic events. This marker may be of major clinical importance, since it would represent the final activation step of the coagulation cascade, and it would be the first marker which is generated exactly at the time of clot formation. In order to support our hypothesis, clinical studies are required which should address the question of clinical relevance as well as aspects of kinetics and stability of the FXIII-AP in plasma samples.

References

1. Shen L, Lorand L. Contribution of fibrin stabilization to clot strength. Supplementation of factor XIII-deficient plasma with the purified zymogen. J Clin Invest 1983; 71: 1336–1341.

2. Sakata Y, Aoki N. Significance of cross-linking of α2-plasmin inhibitor to fibrin in inhibition of fibrinolysis and in hemostasis. J Clin Invest 1982; 69: 536–542.

3. Kohler HP, Stickland MH, Ossei-Gerning N, et al. Association of a common polymorphism in the factor XIII gene with myocardial infarction. Thromb Haemost 1998; 79: 8–13.

4. Kohler HP, Mansfield MW, Clark PS, et al. Interaction between insulin resistance and factor XIII Val34Leu in patients with coronary artery disease. Thromb Haemost 1999; 82: 1202–1203.

5. Kohler HP, Ariens RA, Mansfield MW, et al. Factor XIII activity and antigen levels in patients with coronary artery disease. Thromb Haemost 2001; 85: 569–570.

6. Kucher N, Schroeder V, Kohler HP. Role of blood coagulation factor XIII in patients with acute pulmonary embolism. Correlation of factor XIII antigen levels with pulmonary occlusion rate, fibrinogen, D-dimer, and clot firmness. Thromb Haemost 2003; 90: 434–438.

7. Lorand L. Factor XIII: Structure, activation, and interactions with fibrinogen and fibrin. Ann NY Acad Sci 2001; 936: 291–311.

8. Schwartz ML, Pizzo SV, Hill RL, et al. The subunit structures of human plasma and platelet factor XIII (fibrin-stabilizing factor). J Biol Chem 1971; 246: 5851–5854.

9. Yee VC, Pedersen LC, Le Trong I, et al. Three-dimensional structure of a transglutaminase: Human blood coagulation factor XIII. Proc Natl Acad Sci USA 1994; 91: 7296–7300.

10. Yee VC, Pedersen LC, Bishop PD, et al. Structural evidence that the activation peptide is not released upon thrombin cleavage of factor XIII. Thromb Res 1995; 78: 389–397.

11. Janus TJ, Lewis SD, Lorand L, et al. Promotion of thrombin-catalyzed activation of factor XIII by fibrinogen. Biochemistry 1983; 22: 6269–6272.

12. Ariëns RAS, Philippou H, Chandrasekaran N, et al. The factor XIII V34L polymorphism accelerates thrombin activation of factor XIII and affects cross-linked fibrin structure. Blood 2000; 96: 988–995.

13. Tammen H, Möhring T, Kellmann M, et al. Mass spectrometric phenotyping of Val34Leu polymorphism of blood coagulation factor XIII by differential peptide display. Clin Chem 2004; 50: 545–551.

14. Weiss MS, Metzner HJ, Hilgenfeld R. Two non-proline cis peptide bonds may be important for factor XIII function. FEBS Lett 1998; 423: 291–296.

15. Brooks BR, Bruccoleri RE, Olafson BD, et al. CHARMM: A program for macromolecular energy, minimization, and dynamics calculations. J Comput Chem 1983; 4: 187–217.

16. Lazaridis T, Karplus M. Effective energy function for proteins in solution. Proteins 1999; 35: 133–152.

17. Frishman D, Argos P. Knowledge-based protein secondary structure assignment. Proteins 1995; 23: 566–579.

18. DeLano WL. The PyMOL Molecular Graphics System. 2002; Available at http://www.pymol.org.

19. Humphrey W, Dalke A, Schulten K. VMD: visual molecular dynamics. J Mol Graph 1996; 14: 33–38.

20. Ariëns RAS, Kohler HP, Mansfield MW, et al. Subunit antigen and activity levels of blood coagulation factor XIII in healthy individuals. Relation to sex, age, smoking, and hypertension. Arterioscler Thromb Vasc Biol 1999; 19: 2012–2016.

21. Ferrara P, Caflisch A. Folding simulations of a three-stranded antiparallel beta-sheet peptide. Proc Natl Acad Sci USA 2000; 97: 10780–10785.

22. Ferrara P, Apostolakis J, Caflisch A. Thermodynamics and kinetics of folding of two model peptides investigated by molecular dynamics simulations. J Phys Chem B 2000; 104: 5000–5010.

23. Hiltpold A, Ferrara P, Gsponer J, et al. Free energy surface of the helical peptide $Y(MEARA)_6$. J Phys Chem B 2000; 104: 10080–10086.

24. Ichinose A. The physiology and biochemistry of factor XIII. In: Haemostasis and Thrombosis. Bloom AL, Forbes CD, Thomas DP, Tuddenham EGD, eds. 3rd edn, Vol. 1. Edinburgh: Livingstone. 1994; 531–546.

25. Yorifuji H, Anderson K, Lynch GW, et al. B protein of factor XIII: differentiation between free B and complexed B. Blood 1988; 72: 1645–1650.

26. Hornyak TJ, Bishop PD, Shafer JA. α-Thrombin-catalyzed activation of human platelet factor XIII: relationship between proteolysis and factor XIIIa activity. Biochemistry 1989; 28: 7326–7332.